veloped grids were dried over night, and electron microscopy was carried out with the Philips EM 300 at 80 kV.

Statistic association of developed silver grains to individual fibers was performed with the X^2-method[18] for evaluation. The X^2-distribution gave significance on a 0.1% level for the following statement: helical fibers are radioactively labeled and contain *N*-octyl-[6-^{3}H]-D-gluconamide. Anisotropic sheets (Figure 6a) and rolled up cylinders (Figure 6c) do not contain labeled material. The emulsion covered with unlabeled materials were developed at the same time as the labeled material. We could not detect any silver grain in this blank preparation. More details on sample preparations and analyses will be given in a technical paper.[19]

Differential Scanning Calorimetry. Seventy μL of the micellar solution of several gel mixtures (Table II) were pipetted into suitable pans. The pans were sealed after formation of the gels at room temperature. DSC was carried out by using the Perkin-Elmer DSC-2C calorimeter. Cooling and heating rates were preset at 2.5 deg/min in the temperature range between 280 and 400 K. The values and peak characteristics are given in Table II.

Acknowledgment. This work was supported by the Sonderforschungsbereich 312 "Vectorial Membrane Processes" of the Deutsche Forschungsgemeinschaft, the Förderungskommission of the Freie Universität Berlin, and the Fonds der Chemischen Industrie.

Registry No. D-Glu-8, 18375-61-6; D-Glu-12, 18375-63-8; D-Man-8, 114275-83-1; D-Man-12, 124915-49-7; D-Gal-8, 114275-82-0; D-Gal-12, 124818-97-9; L-Glu-8, 108032-98-0; L-Glu-12, 124818-98-0; L-Man-8, 114275-90-0; L-Man-12, 124818-99-1; L-Gal-8, 114275-89-7; L-Gal-12, 124819-00-7; D[G-^{3}H]Glu-8, 124779-83-5; 1-octanamine, 111-86-4; 1-dodecanamine, 124-22-1; D-[6-^{3}H]glucose, 3615-68-7; D-glucono-δ-lactone, 90-80-2; L-mannono-δ-lactone, 124915-65-7; D-galactono-δ-lactone, 15892-28-1; L-galactono-δ-lactone, 124819-01-8; L-glucose, 921-60-8; D-mannose, 3458-28-4; L-glucono-γ-lactone, 74464-44-1; D-mannono-γ-lactone, 26301-79-1; D-[6-^{3}H]glucono-γ-lactone, 124755-12-0; L-glucono-δ-lactone, 52153-09-0; D-mannono-δ-lactone, 32746-79-5; D-[6-^{3}H]glucono-δ-lactone, 124755-13-1.

(18) Sachs, L. *Statistische Auswertungsmethoden*; Springer Verlag: Berlin, 1968.
(19) Boettcher, C.; Boekema, E.; Fuhrhop, J.-H. Submitted to *J. Microscopy*.
(20) Schnur, J. M.; Price, R.; Schoen, P.; Yager, P.; Calvert, J. M.; Georger, J.; Singh, A. *Thin Solid Films* **1987**, *152*, 181-206.

In Situ Measurement of the Conductivity of Polypyrrole and Poly[1-methyl-3-(pyrrol-1-ylmethyl)pyridinium]$^+$ as a Function of Potential by Mediated Voltammetry. Redox Conduction or Electronic Conduction?

Huanyu Mao and Peter G. Pickup*

Contribution from the Department of Chemistry, Memorial University of Newfoundland, St. John's, Newfoundland, Canada A1B 3X7. *Received June 26, 1989*

Abstract: The electronic conductivity of polypyrrole and poly[1-methyl-3-(pyrrol-1-ylmethyl)pyridinium]$^+$ (poly-MPMP$^+$) films has been investigated by rotating disk voltammetry. In this in situ measurement, a solution redox species such as cobaltocene, ferrocene, or Cr(2,2′-bipyridine)$_3^+$ serves as an electron source at the polymer/solution interface, while electrons are removed at the polymer/electrode interface. The oxidation state of the polymer is controlled by the potential applied to the electrode. The experimental data have been interpreted in terms of both electronic and redox conduction models. A comparison of the results from these two models reveals that the electronic conductivity and the electron diffusion coefficient are related by the Nernst-Einstein equation. It is concluded that electron transport occurs by a hopping mechanism and that the two models are equivalent descriptions of this process in the pyrrole-based polymers. The electronic conductivity of both polymers initially increases linearly with the degree of oxidation of the polymer backbone (concentration of oxidized sites). The conductivity of polypyrrole rises exponentially from 10^{-8} to 5×10^{-6} Ω^{-1} cm^{-1} over the potential range of −0.7 to −0.4 V, while the electron diffusion coefficient remains constant at ca. 10^{-7} cm^2 s^{-1}. At higher potentials the conductivity is too high to be accurately determined by rotating disk voltammetry. The conductivity of poly-MPMP$^+$ increases from ca. 10^{-9} Ω^{-1} cm^{-1} at +0.35 V to ca. 10^{-4} Ω^{-1} cm^{-1} at +1.0 V.

Conducting polymers are currently receiving much attention because of their many potential applications and their intrinsic scientific interest.[1] Of particular interest is the nature and mechanism of electron transport in these materials, which has been investigated extensively by both theoretical and experimental approaches. Most of the experimental studies have focused on dry polymers, although there have been a number of important in situ studies of the electronic conductivity of polymers immersed in an electrolyte solution. The latter type of study is particularly appropriate to the many electrochemical applications of conducting polymers.

In situ (*solvent-wetted*) conductivity measurements on conducting polymers such as polypyrrole, polythiophene, and polyaniline have been made using microelectrode arrays,[2-4] a twin-electrode thin-layer cell,[5] other twin-electrode arrangements,[6,7] and ac impedance spectroscopy.[8] There have also been numerous in situ studies of electron transport through redox polymers, employing techniques such as chronoamperometry,[9] rotating disk

(1) *Handbook of Conducting Polymers*; Skotheim, T. A., Ed.; Marcel Dekker: New York, 1986.
(2) Kittlesen, G. P.; White, H. S.; Wrighton, M. S. *J. Am. Chem. Soc.* **1984**, *106*, 7389-7396.
(3) Paul, E. W.; Ricco, A. J.; Wrighton, M. S. *J. Phys. Chem.* **1985**, *89*, 1441-1447.
(4) Thackeray, J. W.; White, H. S.; Wrighton, M. S. *J. Phys. Chem.* **1985**, *89*, 5133-5140.
(5) Feldman, B. J.; Burgmayer, P.; Murray, R. W. *J. Am. Chem. Soc.* **1985**, *107*, 872-878.
(6) Gholamian, M.; Suresh Kumar, T. N.; Contractor, A. Q. *Proc. Indian Acad. Sci., Chem. Sci.* **1986**, *97*, 457-464.
(7) Focke, W. W.; Wnek, G. E.; Wei, Y. *J. Phys. Chem.* **1987**, *91*, 5813-5818.
(8) Waller, A. M.; Compton, R. G. *J. Chem. Soc., Faraday Trans. I* **1989**, *85*, 977-990.

0002-7863/90/1512-1776$02.50/0

voltammetry,[10] and sandwich electrodes.[11] Electron transport through redox polymers generally occurs by an electron-hopping mechanism and is driven by concentration gradients of oxidized and reduced redox sites.[12,13] This type of conductivity has been termed "redox conductivity" to distinguish it from normal (ohmic) electronic conductivity.[14]

An important recent discovery is that redox conductors can be forced to behave as conventional ohmic conductors if the formation of concentration gradients is prevented. Elliott and co-workers[15] have done this by using an electrolyte solution containing a large polymeric counterion that cannot penetrate the polymer matrix. Murray and co-workers[16,17] used a dry twin-electrode sandwich arrangement. These observations naturally lead to the question of whether concentration gradients and redox conduction are significant in the in situ conductivity of the so-called electronically conducting polymers (e.g., polypyrrole). In a series of elegant experiments employing a twin-electrode sandwich arrangement, Wilbourn and Murray[18] have shown that this is indeed the case for the ladder polymer poly(benzimidazobenzophenanthroline). This polymer is a conventional ohmic conductor when dry but becomes a redox conductor when immersed in an electrolyte solution. Interestingly, the dry polymer is 10^4 times more conductive than when it is wet. In view of these results, it is important that the in situ conductivity of other conducting polymers is carefully examined.

Our interest in the use of pyrrole-based polymers for electrocatalytic applications has prompted us to investigate the in situ conductivity of polypyrrole and the electronically conducting anion-exchange polymer, poly[1-methyl-3-(pyrrol-1-ylmethyl)-pyridinium]$^+$ (poly-MPMP$^+$, I).[19] Poly-MPMP$^+$ is an attractive

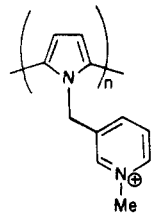

I

material for electrocatalytic applications because it has a high permeability in aqueous electrolyte solutions[20] and it exhibits excellent properties for the binding of multiply charged anionic metal complexes.[19] It is important that its electron-transport properties are fully characterized.

Since we are interested in the ability of these materials to mediate the oxidation of solution species, rotating disk voltammetry is the most appropriate technique with which to investigate their electron-transport properties. Ferrocene, cobaltocene, and Cr(bp)$_3^+$ (bp = 2,2′-bipyridine) were chosen as efficient electron sources that would not diffuse into the polymer matrices. This technique allows us to measure electron-transport rates as a function of potential and is particularly well suited to measurements at very low oxidation (doping) levels. In fact, for polypyrrole, its utility is restricted to oxidation levels below ca. 0.002 holes/pyrrole. The rotating disk technique has previously been used to investigate electron transport through both redox polymers[10,21,22] and conducting polymers.[23-25]

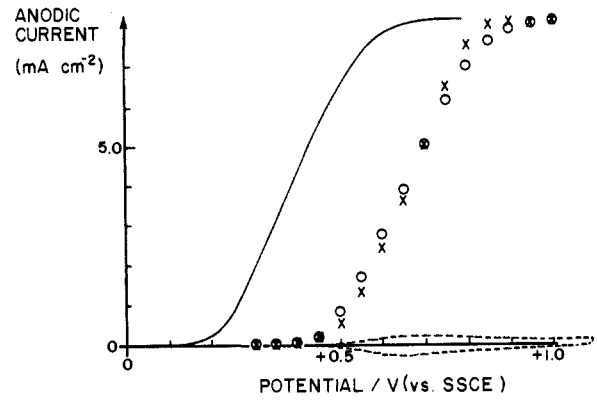

Figure 1. Rotating disk voltammograms (2000 rpm) for oxidation of ferrocene (5.0 mM in CH_3CN + 0.1 M $LiClO_4$) at a naked Pt electrode (—, scan speed = 10 mV s^{-1}) and at a poly-MPMP$^+$- (0.70-μm) coated Pt electrode (× forward scan, o cathodic scan; current measured after 20 s at each potential). The dashed line is a cyclic voltammogram (10 mV s^{-1}) of a poly-MPMP$^+$- (0.70-μm) coated Pt electrode in CH_3CN + 0.1 M $LiClO_4$ (same current scale).

Experimental Section

Electrochemistry. Electrochemical experiments were carried out in conventional three-compartment glass cells under an argon atmosphere at 23 ± 2 °C. Three or four electrode arrangements consisting of a 0.458-cm^2 Pt rotating disk electrode (RDE) sealed in PTFE (Pine Instruments), a mercury pool electrode [for experiments involving cobaltocene or Cr(bp)$_3^+$], a Pt wire counter electrode, and a saturated sodium chloride calomel electrode (SSCE) reference electrode were used. All potentials are quoted with respect to the SSCE. The potentials of the Pt working electrode and the mercury pool were independently controlled by a Pine Instruments RDE4 potentiostat/galvanostat. A BBC MDL780 X-Y recorder and a Pine Instruments ASR electrode rotator were also used.

Chemicals. 1-Methyl-3-(pyrrol-1-ylmethyl)pyridinium tetrafluoroborate (MPMPBF$_4$) was prepared as previously described.[19] Cr(bp)$_3^+$ was prepared in situ as follows. $CrCl_3 \cdot 6H_2O$ (0.59 g, Fisher) and 2,2′-bipyridine (0.82 g, Aldrich) in water (20 mL) were boiled for 5 min before addition of $NaClO_4$ (1.6 g). The crude Cr(III)–bipyridine product that crystallized on cooling was reduced in CH_3CN at a mercury pool electrode at −1 V to give a mixture of Cr(bp)$_3^+$ and Cr(bp)$_3^{2+}$.

Pyrrole (Aldrich) was purified on a dry alumina column. Ferrocene (Aldrich), cobaltocenium hexafluorophosphate (Aldrich), tetraethylammonium perchlorate (TEAP, Fluka), tetraethylammonium tetrafluoroborate (TEABF$_4$, Fluka), lithium perchlorate (Fluka), and acetonitrile (Fisher, HPLC grade) were used as received.

Preparation of Polymer Films. Pyrrole was electrochemically polymerized at a constant current density of 0.33 mA cm^{-2} from 0.1 M pyrrole in acetonitrile containing 0.1 M TEAP. A charge density of 0.24 C cm^{-2} is assumed to produce a 1.0 μm thick film.[26] MPMPBF$_4$ was polymerized from 0.05 M acetonitrile solutions containing 0.1 M TEABF$_4$ at a constant current density of 0.8 mA cm^{-2}. A charge density of 0.15 C cm^{-2} produces a 1.0 μm thick polymer film.[19]

Results

Ferrocene Oxidation at Poly-MPMP$^+$-Coated Electrodes. Rotating disk voltammograms of 5.0 mM ferrocene in acetonitrile at naked Pt and poly-MPMP$^+$-coated electrodes are shown in

(9) Daum, P.; Lenhard, J. R.; Rolison, D.; Murray, R. W. *J. Am. Chem. Soc.* **1980**, *102*, 4649–4653.
(10) Ikeda, T.; Leidner, C. R.; Murray, R. W. *J. Electroanal. Chem.* **1982**, *138*, 343–365.
(11) Pickup, P. G.; Kutner, W.; Leidner, C. R.; Murray, R. W. *J. Am. Chem. Soc.* **1984**, *106*, 1991–1998.
(12) Kaufman, F. B.; Schroeder, A. H.; Engler, E. M.; Kramer, S. R.; Chambers, J. Q. *J. Am. Chem. Soc.* **1980**, *102*, 483–487.
(13) Chidsey, C. E. D.; Murray, R. W. *Science* **1986**, *231*, 25–31.
(14) Pickup, P. G.; Murray, R. W. *J. Am. Chem. Soc.* **1983**, *105*, 4510–4514.
(15) Elliott, C. M.; Redepenning, J. G.; Balk, E. M. *J. Am. Chem. Soc.* **1985**, *107*, 8302–8304.
(16) Jernigan, J. C.; Murray, R. W. *J. Phys. Chem.* **1987**, *91*, 2030–2032.
(17) Jernigan, J. C.; Surridge, N. A.; Zvanut, M. E.; Silver, M.; Murray, R. W. *J. Phys. Chem.* **1989**, *93*, 4620–4627.
(18) Wilbourn, K.; Murray, R. W. *J. Phys. Chem.* **1988**, *92*, 3642–3648.
(19) Mao, H.; Pickup, P. G. *J. Electroanal. Chem.* **1989**, *265*, 127–142.
(20) Mao, H.; Pickup, P. G. *J. Phys. Chem.* **1989**, *93*, 6480–6485.
(21) Pickup, P. G.; Osteryoung, R. A. *J. Electroanal. Chem.* **1985**, *186*, 99–111.
(22) Turner Jones, E. T.; Faulkner, L. R. *J. Electroanal. Chem.* **1987**, *222*, 201–222.
(23) Pickup, P. G.; Osteryoung, R. A. *J. Electroanal. Chem.* **1985**, *195*, 271–288.
(24) Genies, E. M.; Tsintavis, C. *J. Electroanal. Chem.* **1986**, *200*, 127–145.
(25) Rault-Berthelot, J.; Orliac, M.-A.; Simonet, J. *Electrochim. Acta* **1988**, *33*, 811–823.
(26) Bull, R. A.; Fan, F.-R. F.; Bard, A. J. *J. Electrochem. Soc.* **1982**, *129*, 1009–1015.

Figure 1. The polymer coating shifts the half-wave potential for ferrocene oxidation to higher potential by ca. 180 mV in this case. The absence of an oxidation wave close to the formal potential of ferrocene (ca. +0.43 V) indicates that ferrocene does not diffuse through the polymer film to the underlying Pt electrode. We have seen no evidence for ferrocene permeation even for films as thin as 35 nm. The ferrocene oxidation currents observed at the poly-MPMP$^+$-coated electrode must therefore be due to electron transfer from ferrocene to the outer surface of the polymer. Under these circumstances the current in the rotating disk voltammogram can be limited by mass transport of ferrocene to the polymer, electron transport through the polymer, the kinetics of the electron-transfer steps or some combination of these processes.[27-29]

In all cases studied in this work, the limiting current at the polymer-coated electrode was the same as that at a bare Pt electrode. This indicates that, at sufficiently high potentials, the polymer films become sufficiently conductive that the current is limited by mass transport of the ferrocene to the polymer surface. However, on the rising portion of the wave (below ca. 80% of the limiting current), the current is independent of the substrate concentration and the electrode rotation rate, but decreases with increasing film thickness. These observations show that the current in this region is limited by the rate of electron transport across the polymer film. This corresponds to the $S - t_e$ and E cases in Albery's[27] and Saveant's[29] theoretical treatments, respectively.

It was suggested by a reviewer that the film may become permeable to ferrocene when it begins to be oxidized. However, it is unlikely that poly-MPMP$^+$, which already contains a cationic site concentration of over 5 M when reduced, would swell significantly when oxidized. Further, we have found that the diffusion coefficient of ClO_4^- in oxidized poly-MPMP$^+$ (1.1×10^{-9} cm^2 s^{-1}) is not significantly greater than that of I^- in reduced poly-MPMP$^+$ (5.4×10^{-10} cm^2 s^{-1}).[30]

As can be seen from the voltammogram shown in Figure 1, the ferrocene oxidation current at the polymer-coated electrode rises sharply as the polymer begins to be oxidized. This increasing current reflects the increasing conductivity of the polymer film. However, as the current approaches its limiting value, it begins to be limited by the mass-transport rate, and no further information can be obtained concerning the polymer conductivity. Thus, each polymer film can only yield conductivity data over a potential range of ca. 300 mV. To cover a wider range, a number of films ranging in thickness from 35 nm to 6 μm were used. Each film exhibited a ferrocene oxidation wave shaped similarly to that shown in Figure 1, with the half-wave potential shifting progressively to higher potentials as the film thickness was increased.

Cobaltocene Oxidation at Polypyrrole-Coated Electrodes. It is difficult to obtain conductivity data for polypyrrole by rotating disk voltammetry of ferrocene because the conductivity of the polymer is very high (>10^{-2} Ω^{-1} cm^{-1}) at potentials at which ferrocene is oxidized.[23] Instead, cobaltocene ($E^{\circ\prime} = -0.98$ V) in acetonitrile was used. Cobaltocene was produced in situ by electrochemical reduction of cobaltocenium hexafluorophosphate at a mercury pool electrode. The mercury pool was generally maintained at −1.2 V throughout the experiment to regenerate cobaltocene consumed at the RDE. It was essential that oxygen was rigorously excluded from the cell since it resulted in immediate decomposition of the cobaltocene.

An example of rotating disk voltammetry of cobaltocene at a polypyrrole-coated electrode is shown in Figure 2. The oxidation is shifted from the reversible half-wave potential (−0.98 V) to the potential region in which the polymer becomes conductive. Thus, reduced polypyrrole is impermeable to cobaltocene. The possibility that polypyrrole becomes permeable to cobaltocene as it is oxidized is extremely unlikely. The diffusion coefficient of ClO_4^- in fully

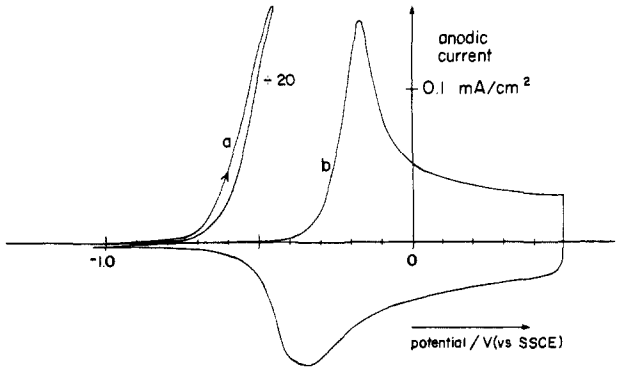

Figure 2. a. Rotating disk voltammogram (5 mV s^{-1}, 1000 rpm) for cobaltocene (2 mM in CH_3CN + 0.1 M TEAP) oxidation at a polypyrrole- (0.14-μm) coated Pt electrode. b. Cyclic voltammogram (10 mV s^{-1}) of a polypyrrole- (0.14-μm) coated Pt electrode in CH_3CN + 0.1 M TEAP.

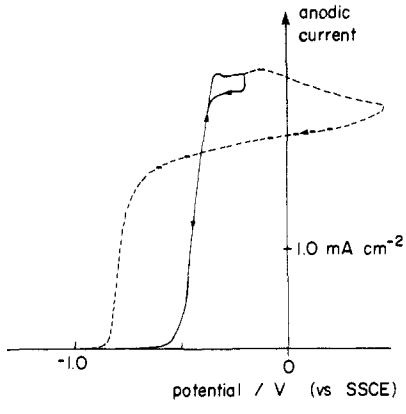

Figure 3. Rotating disk voltammograms (2 mV s^{-1}, 1000 rpm) for cobaltocene (2 mM in CH_3CN + 0.1 M TEAP) oxidation at a polypyrrole- (1.5-μm) coated Pt electrode. (–) first scan, (---) second scan.

oxidized polypyrrole (1.0×10^{-9} cm^2 s^{-1} for film thickness of <2 μm) is not significantly greater than that of I^- in reduced poly-MPMP$^+$ (5.4×10^{-10} cm^2 s^{-1}),[30] which we have shown to be impermeable to ferrocene. The independence of the mediated current (below 80% of its limiting value) on rotation rate is further evidence that permeation is not a significant factor in these experiments.

Contrary to the case of ferrocene oxidation at poly-MPMP$^+$, significant hysteresis was observed between the forward and reverse scans under some circumstances. An example of this is shown in Figure 3. The forward and reverse scans coincide when the polymer is not oxidized to a significant extent, but extending the potential scan to fully oxidize the film results in an extended conductive region on the cathodic scan. This not a simple kinetic effect since similar behavior was observed at scan speeds of 2 and 10 mV s^{-1}. Presumably the oxidized form of the polymer undergoes a structural change that decreases its reduction potential. This change in reduction potential is also reflected in cyclic voltammetry of polypyrrole (e.g., Figure 2) and has been recently discussed by Feldberg and Rubinstein[31] and by Albery et al.[32] The hysteresis at potentials above −0.4 V in the rotating disk voltammograms shown in Figure 3 is due to oxidation and reduction of the polymer, which is superimposed on the limiting current due to colbaltocene oxidation. The current slowly decreases during the extended scan (---) because of depletion of cobaltocene in the bulk solution (volume, ~8 mL). The observation of an increasing current for reduction of cobaltocenium at the mercury pool electrode supports this explanation.

(27) Albery, W. J.; Hillman, A. R. *Ann. Rep. Prog. Chem., Sect. C* **1981**, 377–437.
(28) Rocklin, R. D.; Murray, R. W. *J. Phys. Chem.* **1981**, *85*, 2104–2112.
(29) Andrieux, C. P.; Dumas-Bouchiat, J. M.; Saveant, J.-M. *J. Electroanal. Chem.* **1982**, *131*, 1–35.
(30) Mao, H.; Ochmanska, J.; Paulse, C. D.; Pickup, P. G. *Faraday Discuss. Chem. Soc.*, in press.
(31) Feldberg, S. W.; Rubinstein, I. *J. Electroanal. Chem.* **1988**, *240*, 1–15.
(32) Albery, W. J.; Chen, Z.; Horrocks, B. R.; Mount, A. R.; Wilson, P. J.; Bloor, D.; Monkman, A. T.; Elliott, C. M. *Faraday Discuss. Chem. Soc.*, in press.

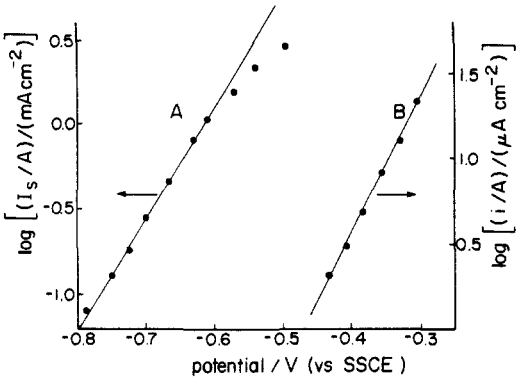

Figure 4. log current vs potential plots for (A) the cobaltocene oxidation rotating disk voltammogram (the steady-state current at each potential was used) and (B) the anodic rising portion of the cyclic voltammogram, shown in Figure 2.

Table I. Slopes of log Current vs Potential Plots (e.g., Figure 4) for Voltammetric Oxidation of Polypyrrole (CV) and Cobaltocene at a Rotating Polypyrrole-Coated Electrode (RDV)[a]

film thickness/μm	slope/V decade^{-1}	
	CV	RDV
0.14	0.12 (−0.43 to −0.30 V)	0.15 (−0.80 to −0.60 V)
0.14	0.14 (−0.38 to −0.30 V)	
0.50		0.12 (−0.70 to −0.50 V)
1.5	0.15 (−0.50 to −0.35 V)	0.10 (−0.60 to −0.40 V)

[a] Potential range in parentheses.

The maximum oxidation level at which conductivity data for polypyrrole was obtained in these experiments was ca. 0.002 holes/pyrrole (at −0.4 V). This limit can presumably be extended by using thicker films, higher cobaltocene concentrations, and higher rotation rates.

Theory

It is clear from the voltammograms shown in Figures 1–3 that the in situ conductivities of both polypyrrole and poly-MPMP$^+$ increase sharply with increasing potential as they are oxidized. The initial functional dependence on potential of the current both for mediated oxidation of solution species (I_s) and for oxidation of the polymers themselves is exponential. This is demonstrated in Figure 4 where log current vs potential plots for the voltammetric oxidation of polypyrrole and the mediated oxidation of cobaltocene by polypyrrole, in the region of the initial increase, are shown. The slopes of these plots and of similar plots for other polypyrrole films are presented in Table I. Within experimental error, the slopes for these two types of experiment are the same (average = 0.13 ± 0.02), indicating that the cobaltocene oxidation current is proportional to the level of oxidation of the polymer. Errors associated with these slopes can arise from background currents and from leveling of the plots as the current approaches either the peak or limiting current. Some variation in the slopes is also due to activity effects that lead to different Nernstian slopes at different potentials from $E^{\circ\prime}$.[33]

Thus, the conductivity of polypyrrole (related to the cobaltocene oxidation current) increases exponentially with potential and appears to be proportional to the charge on the polypyrrole backbone (integral of the polypyrrole oxidation current under a cyclic voltammogram), which is reasonable. Similar relationships apply for poly-MPMP$^+$. In the following sections we examine the rotating electrode data in terms of both electronic and redox conductivity models.

(a) Electronic Conductivity Model. On the basis of the above evidence, we can empirically express the conductivity of either polymer ($\sigma(E)$) as a function of potential by

$$\sigma(E) = \sigma_0 e^{(E-E_0)/s} \tag{1}$$

(33) Albery, W. J.; Boutelle, M. G.; Colby, P. J.; Hillman, A. R. *J. Electroanal. Chem.* **1982**, *133*, 135–145.

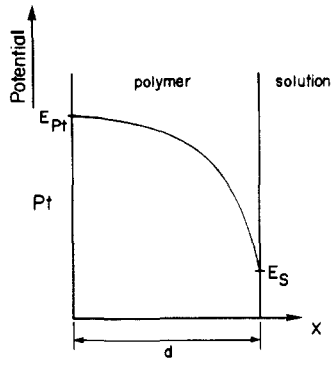

Figure 5. Schematic diagram of the steady-state potential profile across a conducting polymer film during the mediated oxidation of a solution species.

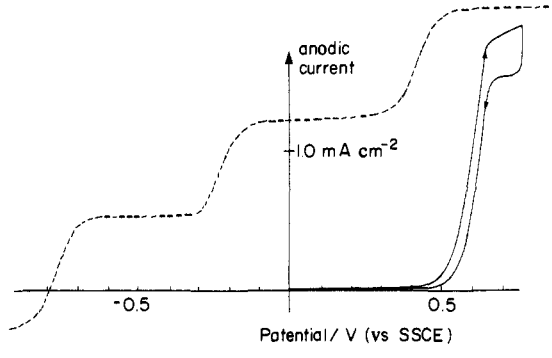

Figure 6. Rotating disk voltammograms (10 mV s^{-1}, 1000 rpm) for oxidation of a mixture of $Cr(bp)_3^+$ (1 mM), $Cr(bp)_3^{2+}$ (0.3 mM), and ferrocene (0.6 mM) in CH_3CN + 0.1 M $TEABF_4$ at naked Pt (---) and poly-MPMP$^+$- (0.35-μm) coated Pt (—) electrodes.

where σ_0 is the conductivity at some arbitrary potential E_0, and $2.303s$ is the empirical slope of a log I_s vs potential plot (Table I). In the rotating electrode experiments, the conductivity of the polymer film is highest close to the Pt electrode surface (which is at a higher potential than the outer surface of the polymer) and decreases sharply across the film. The potential profile across the film is shown schematically in Figure 5. E_{Pt} is the potential set by the potentiostat and E_s is the potential established at the polymer/solution interface by the dissolved redox couple. E_s is the same as the potential at a bare electrode at the same current and under identical mass-transport conditions.

The current for the mediated oxidation (I_s) will be given by

$$I_s = \frac{dE(x)}{R(x)} = A\sigma(E)\frac{dE(x)}{dx} \tag{2}$$

where $dE(x)$ is the potential difference across an infinitely thin layer of film a distance x from the underlying Pt electrode, and $R(x)$ is the resistance of this layer. Combination of eq 1 and 2 and integration between E_s and E_{Pt} thus

$$d = \int_{E_s}^{E_{Pt}} \frac{A\sigma_0 e^{(E-E_0)/s}}{I_s}\,dE \tag{3}$$

where d is the thickness of the film, yields

$$\sigma_0 = \frac{I_s d}{sA(e^{(E_{Pt}-E_0)/s} - e^{(E_s-E_0)/s})} \tag{4}$$

If we let $E_0 = E_{Pt}$ and if $E_{Pt} \gg E_s$, then eq 4 reduces to

$$\sigma(E_{Pt}) = I_s d/sA \tag{5}$$

Equation 5 predicts that the mediated current at any particular potential will be independent of E_s and thus independent of the redox potential of the species being oxidized (as long as E_{Pt} is at least several hundred millivolts positive of E_s). This surprising result was tested by simultaneous oxidation of $Cr(bp)_3^+$ and ferrocene at a rotating poly-MPMP$^+$-coated electrode. Voltam-

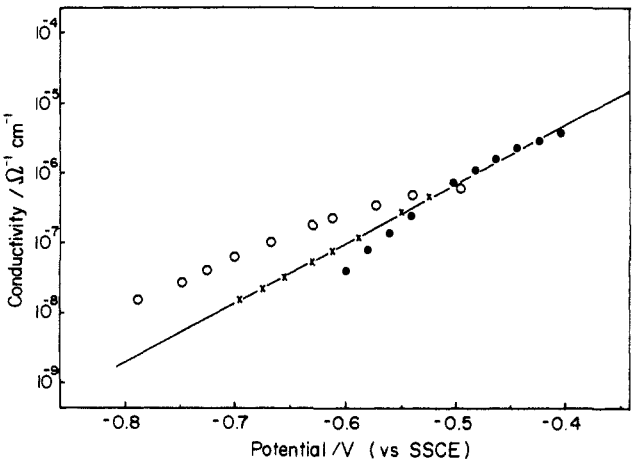

Figure 7. Conductivity vs potential for polypyrrole in acetonitrile + 0.1 M TEAP, from rotating disk voltammetry of cobaltocene using eq 5. Film thicknesses: 0.14 (○), 0.50 (×), and 1.5 (●) μm. The line represents the average slope of 120 mV/decade for the three sets of data.

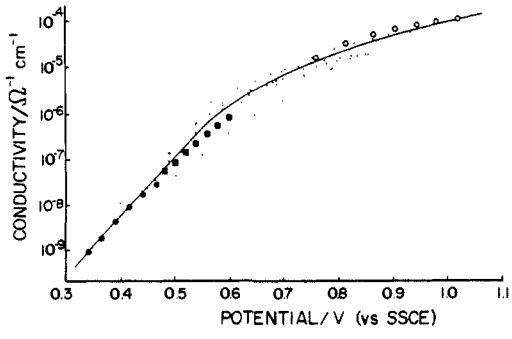

Figure 8. Conductivity vs potential for poly-MPMP$^+$ in acetonitrile + 0.1 M $TEABF_4$ or 0.1 M $LiClO_4$, from rotating disk voltammetry of ferrocene using eq 5. Film thicknesses: 35 nm (●) ($LiClO_4$), 0.35 μm (■) [$TEABF_4$ + $Cr(bp)_3^{2+/+}$ (see Figure 6)], 6.0 μm (○) ($LiClO_4$), and seven other films from 0.35 to 3.0 μm (·); 90 mV has been added to all potentials measured in 0.1 M $LiClO_4$ to account for the difference in junction potential.

mograms obtained at bare and coated electrodes are shown in Figure 6. The final limiting current is lower at the coated electrode because some oxygen entered the cell when the electrode was changed. This was confirmed by subsequently replacing the coated electrode with the bare electrode, which resulted in a further decrease in the final limiting current. It should be noted that this decrease in limiting current is not indicative of a breakdown of the validity of eq 5. The limiting currents in all experiments described in this paper are determined by the mass-transport rate of the solution species. None of the equations that we use apply to the limiting region of the RDV.

In the experiment represented by Figure 6, E_s changes abruptly at the $Cr(bp)_3^{2+/+}$ limiting current (ca. 0.5 mA cm^{-2}) and again at the $Cr(bp)_3^{3+/2+}$ limiting current (ca. 1.2 mA cm^{-2}). The absence of sharp changes in potential at these currents at the poly-MPMP$^+$-coated electrode clearly shows that the mediated current is independent of E_s as predicted by eq 5. Further, the data from this experiment are in excellent quantitative agreement with data from experiments using ferrocene alone (Figure 8), despite the large difference in E_s at currents below 1.2 mA cm^{-2}.

Equation 5 was used to calculate conductivity as a function of potential for both polypyrrole and poly-MPMP$^+$ from mediated oxidation experiments at electrodes coated with films of varying thickness. These results are presented in Figures 7 and 8. The results for polypyrrole (Figure 7) show that its conductivity increases exponentially from ca. 1×10^{-8} Ω^{-1} cm^{-1} at −0.7 V to ca. 5×10^{-6} Ω^{-1} cm^{-1} at −0.4 V. The value of ca. 10^{-7} Ω^{-1} cm^{-1} at −0.6 V agrees with that reported by Murray and co-workers.[5] The systematic deviation of the three sets of data at low potential suggests that the conductivity of polypyrrole becomes thickness

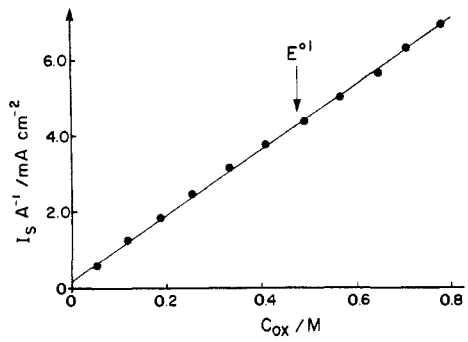

Figure 9. Steady-state current vs concentration of oxidized polymer sites for the oxidation of ferrocene (5.0 mM in CH_3CN + 0.1 M $LiClO_4$) at a rotating (2000 rpm) poly-MPMP$^+$- (1.0-μm) coated Pt electrode.

dependent in this region. However, this is probably a consequence of failure of the thicker films to reach full equilibrium in the time scale of the measurements (20 s per point for the 1.5-μm film). Albery et al.[32] have recently shown that lightly oxidized polypyrrole can exist in a metastable state for several minutes. Thus, our results for the thickest film may reflect the conductivity of this metastable state while those for the thinnest film correspond to the equilibrium state. At higher potentials the metastable state becomes increasingly unstable[32] and so the results for the three films merge.

These experiments were much easier to peform with poly-MPMP$^+$ and consequently a larger data set and better reproducibility were obtained. Data for 10 films ranging in thickness from 35 nm to 6 μm are shown in Figure 8. These experiments were performed with either $TEABF_4$ or $LiClO_4$ as the electrolyte. However, after correction for the difference in junction potential (based on the formal potential of ferrocene) no significant differences were observed. As can be seen from Figure 8, the conductivity of poly-MPMP$^+$ rises exponentially from ca. 10^{-9} Ω^{-1} cm^{-1} at 0.35 V to ca. 10^{-6} Ω^{-1} cm^{-1} at 0.6 V with a slope of ca. 90 mV per decade. At potentials above 0.6 V, the conductivity begins to level off as the formal potential of the polymer (0.74 V) is approached and the increase in oxidation level of the polymer with potential ceases to be exponential. In this region, eq 5 ceases to be rigorous and begins to overestimate the conductivity. Thus, the data in Figure 8 for potentials above 0.6 V should be regarded as semiquantitative. The maximum electronic conductivity of poly-MPMP$^+$, estimated here to be ca. 10^{-4} Ω^{-1} cm^{-1} (Figure 8), agrees with our chronoamperometric and dry conductivity measurements.[30] This is an order of magnitude higher than a value that we originally reported,[19] which we now believe to be an underestimate.

(b) Redox Conductivity Model. In the most simple treatment of redox conductivity under steady-state conditions, a linear concentration gradient of oxidized (or reduced) sites is assumed to exist across the film. For the mediated oxidation of a solution species, the concentration of oxidized sites at the electrode/polymer interface is controlled by the applied potential (E_{Pt}) according to the Nernst equation. The concentration at the polymer/solution interface can be assumed to be zero if the formal potential of the solution species is significantly less than that of the polymer.

Under these assumptions, the steady-state oxidation current is given by[28]

$$I_s = FAD_eC_{ox}/d \qquad (6)$$

were D_e is the electron diffusion coefficient, and C_{ox} is the concentration of oxidized sites at the polymer/electrode interface. C_{ox} can be evaluated at different potentials from the charge under a voltammogram of the polymer integrated to that potential [$C_{ox}(E) = Q(E)/FAd$].

For poly-MPMP$^+$ films in the thickness range 0.35–1.0 μm, plots of I_s (for mediated ferrocene oxidation) vs C_{ox} were linear (e.g., Figure 9) as predicted by eq 6. Diffusion coefficients from these plots are presented in Table II. Thicker films (3.0 and 6.0 μm), which produced data predominantly at potentials above the voltammetric peak potential of poly-MPMP$^+$, gave nonlinear plots

Table II. Electron Diffusion Coefficients (D_e) in Poly-MPMP$^+$ from Rotating Disk Voltammetry of Ferrocene at Poly-MPMP$^+$-Coated Electrodes

film thickness/μm	electrolyte	$D_e/10^{-9}$ cm^2 s^{-1} eqs 6 and 7	eq 6
0.035	$LiClO_4$	2.6	
0.35[a]	$TEABF_4$	4.9	
0.35	$TEABF_4$	2.1	4.2
0.70	$LiClO_4$	11.4	9.0
0.70	$LiClO_4$	4.5	6.3
0.70	$LiClO_4$	4.1	5.9
1.0	$TEABF_4$	6.2	9.1
1.0	$LiClO_4$	7.2	9.9

[a] Ferrocene + $Cr(bp)_3^{2+/+}$ (see Figure 6).

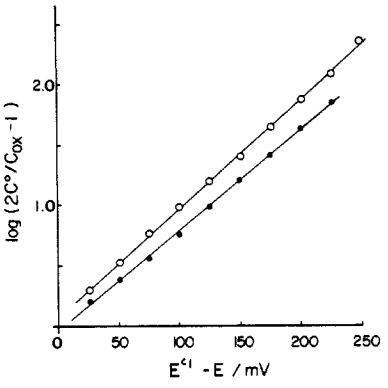

Figure 10. log $(2C^\circ/C_{ox} - 1)$ vs $(E^{\circ\prime} - E)$ for polypyrrole (0.14 μm) in CH_3CN + 0.1 M TEAP (O) and for poly-MPMP$^+$ (0.35 μm) in CH_3CN + 0.1 M $TEABF_4$ (●).

whose slopes increased with increasing C_{ox}. This suggests that D_e begins to increase with increasing C_{ox} in this region of potential. Thus it appears that the so called capacitive process for poly-MPMP$^+$, at potentials positive of $E^{\circ\prime}$, produces more mobile oxidized sites than those produced during the main redox process. Another way of viewing this is that bipolaron states formed at high potentials are more mobile than polaron states.

Data for thinner poly-MPMP$^+$ films and for polypyrrole films (mediating cobaltocene oxidation) were more difficult to analyze because direct determination of C_{ox} at the low potentials covered by these data was not accurate. Instead, C_{ox} values were estimated by extrapolation of a semiempirical C_{ox} vs potential function. For potentials less than $E^{\circ\prime}$, the dependence of C_{ox} on potential for polypyrrole and poly-MPMP$^+$ can be represented by the following form of the Nernst equation.

$$C_{ox} = 2C^\circ/(1 + \exp[f(E^{\circ\prime} - E)]) \quad (7)$$

where $E^{\circ\prime}$ is the formal potential of the polymer, C° is the concentration of oxidized sites in the polymer at $E^{\circ\prime}$, and $f = gF/RT$. (For a redox polymer, C° is equal to half of the total redox site concentration). We have added an additional parameter, g, to the Nernst slope to account for activity effects.[33] The validity of eq 7 is demonstrated in Figure 10, where log $(2C^\circ/C_{ox} - 1)$ values determined by cyclic voltammetry are plotted against $E^{\circ\prime} - E$. Linear plots are obtained for both polypyrrole and poly-MPMP$^+$. The average slopes of these plots for two films of each type (103 and 117 mV, respectively) yielded g values of 0.57 for polypyrrole and 0.50 for poly-MPMP$^+$.

Some clarification of how the data in Figure 10 were determined is required. Since polypyrrole appears to have different formal potentials for reduction and oxidation, and our rotating disk data are for the reduced form, we have defined $E^{\circ\prime}$ for polypyrrole as the anodic peak potential for a slow cyclic voltammogram (−0.18 V). C_{ox} values for polypyrrole were determined solely from anodic voltammetric scans. No such difference between the two oxidation states exists for poly-MPMP$^+$ and so we have defined $E^{\circ\prime}$ for this polymer as the average of the anodic and cathodic peak potentials in cyclic voltammetry (+0.74 V). C_{ox} values were calculated from average charges under the anodic and cathodic parts of voltammograms. The average C° values determined by cyclic voltammetry were 0.9 M for polypyrrole and 0.6 M for poly-MPMP$^+$.

Table III. Electron Diffusion Coefficients (D_e) in Polypyrrole from Rotating Disk Voltammetry of Cobaltocene at Polypyrrole-Coated Electrodes

film thickness/μm	$D_e/10^{-7}$ cm^2 s^{-1}
0.14	3.2
0.50	1.1
1.5	1.2

Electron diffusion coefficients for poly-MPMP$^+$ and polypyrrole films, determined by using eq 6 and 7, are presented in Tables II and III, respectively. For poly-MPMP$^+$ the diffusion coefficients obtained with the use of eq 7 are in good agreement with those obtained from directly determined C_{ox} values. Equation 7 clearly provides an acceptable method for extrapolation to potentials at which C_{ox} can not satisfactorily be directly determined. D_e for poly-MPMP$^+$ was determined with good reproducibility, with the average value being $(6.1 \pm 2.9) \times 10^{-9}$ cm^2 s^{-1}.

There is some difficulty in the estimation of D_e for polypyrrole because of uncertainty in the value of g. The result is very sensitive to this parameter because all data for polypyrrole were obtained at potentials far from $E^{\circ\prime}$. The diffusion coefficients presented in Table III were obtained by using a g value of 0.49, which represents the average slope (120 mV) of the three sets of data in Figure 7. This value of g was chosen primarily because it yields approximately linear I_S vs C_{ox} plots and consistent D_e values for the three films studied. It is in fair agreement with the value of 0.57 obtained from log $(2C^\circ/C_{ox} - 1)$ vs E plots (see above). Thus we can conclude that the electron diffusion coefficient in lightly oxidized polypyrrole is ca. 10^{-7} cm^2 s^{-1}.

Discussion

In this work the potential dependence of the in situ electronic conductivity of polypyrrole and poly-MPMP$^+$ has been adequately described by using both electronic and redox conduction models. In the electronic conduction model the electron-transport rate is determined by a potential-dependent conductivity parameter, σ, while in the redox conduction model the relevant parameter is the electron diffusion coefficient, D_e. The question now to be answered is which of these parameters provides the more realistic description of the electron-transport process—or are both appropriate.

A relationship between σ and D_e can be obtained by combining eq 5 and 6.

$$I_s = sA\sigma/d = FAD_eC_{ox}/d$$

Since empirical values of s are similar to values of RT/gF, it is reasonable to equate these two exponential slopes. We then obtain

$$\sigma = gF^2D_eC_{ox}/RT \quad (8)$$

which is a form of the Nernst–Einstein equation relating the mobility of a charged species to its diffusion coefficient. The g factor (ca. 0.5) accounts for the fact that the activity of oxidized sites in the polymer is lower than their concentration.

The applicability of the Nernst–Einstein equation to electron transport through the polymers studied here implies that this transport occurs by an electron-hopping mechanism between localized sites.[34,35] This is in agreement with recent views of electron transport in polypyrrole.[36,37] The localized sites presumably consist of conjugated segments of polymer that are separated by defects.[38]

(34) Saveant, J. M. *J. Electroanal. Chem.* **1988**, *242*, 1–21.
(35) Focke, W. W.; Wnek, G. E. *J. Electroanal. Chem.* **1988**, *256*, 343–352.
(36) Pfluger, P.; Weiser, G.; Scott, J. C.; Street, G. B. In *Handbook of Conducting Polymers*; Skotheim, T. A., Ed.; Marcel Dekker: New York, 1986; Vol. 2, pp 1369–1381.
(37) Bredas, J. L.; Street, G. B. *Acc. Chem. Res.* **1985**, *18*, 309–315.
(38) Diaz, A. F.; Crowley, J.; Bargon, J.; Gardini, G. P.; Torrance, J. B. *J. Electroanal. Chem.* **1981**, *121*, 355–361.

Equation 8 has been obtained here based on the observation that the conductivities of the polymers studied increase exponentially with potential. This is only true for potentials at least 100 mV negative of $E^{\circ\prime}$ and so the general validity of eq 8 still remains to be established. At more positive potentials eq 5 overestimates σ. However, under these circumstances the effective charge carrier concentration (C_{cc}) becomes less than C_{ox} since the number of available sites for electrons to hop from (or holes to hop to) is smaller.[39] A more general relationship between σ and D_e is thus[39]

$$\sigma = gF^2D_eC_{cc}/RT \tag{9}$$

where

$$C_{cc} = C_{ox}C_{red}/(C_{ox} + C_{red}) \tag{10}$$

An analogous expression was derived by Dahms for electron hopping in solution.[40] Equation 9 is equivalent to eq 8 for $E \ll E^{\circ\prime}$. Unfortunately, we cannot use eq 9 here, because we cannot determine C_{red} (the concentration of reduced polymer sites) for polypyrrole or poly-MPMP$^+$. These polymers are significantly less than 50% oxidized at $E^{\circ\prime}$ (see Figures 1 and 2), and so $C_{ox} + C_{red}$ is significantly greater than $2C^{\circ}$.

Since eq 5 is based on the empirical relationship represented by eq 1, we have empirically shown that the electronic conductivity of polypyrrole (and poly-MPMP$^+$) is related to its electron diffusion coefficient by the Nernst–Einstein equation. Since this is the expected theoretical relationship for an electron-hopping mechanism, we can conclude that, for these polymers, the electronic and redox conduction models are equivalent descriptions of electron transport. The in situ conductivity of these polymers can thus be described either as a potential-dependent conductivity (σ) or as an electron diffusion coefficient (D_e), depending on which is most convenient. In many cases the redox description will be most appropriate because D_e is generally independent of potential.

The redox description of polypyrrole conduction is useful for comparisons between the electron-transport properties of conducting polymers and redox polymers. Poly[Os(bp)$_2$(vpy)$_2$]$^{n+}$ (vpy = 4-vinylpyridine), a typical redox polymer whose electron-transport properties have been extensively studied, exhibits electron diffusion coefficients of 8×10^{-9}, 2×10^{-8}, and 2×10^{-7} cm^2 s^{-1} for the 3+/2+, 2+/1+, and 1+/0 couples, respectively.[11] In this paper, we have estimated D_e to be ca. 10^{-7} cm^2 s^{-1} for polypyrrole and 6×10^{-9} cm^2 s^{-1} for poly-MPMP$^+$. Thus, poly-MPMP$^+$ exhibits an electron mobility similar to that of a good redox polymer while the 1+/0 mixed-valent state of poly[Os(bp)$_2$(vpy)$_2$]$^{n+}$ exhibits an electron mobility similar to that of a good electronically conducting polymer. No rigorous distinction between redox and conducting polymers can therefore be made on the basis of the magnitude of their electronic conductivity.

Since our results indicate that electron conduction by polypyrroles is not fundamentally different from electron conduction in redox polymers, we now attempt to explain the apparent differences between ohmic and redox conduction.

The apparent changes between electronic and redox conduction described in the introduction of this paper may merely be the consequence of different potential profiles across the film. If the counterions in the polymer are immobile, the concentrations of oxidized and reduced sites remain constant across the film when a potential difference is applied, a linear potential profile is obtained, and ohmic behavior is observed. If the counterions are mobile, however, the concentrations of oxidized and reduced sites change across the film when a potential difference is applied. Since the effective charge carrier concentration is a function of these concentrations, it too, and hence the polymer conductivity, changes across the film. This results in a nonlinear potential profile (e.g., Figure 5). Electron hopping in this type of varying field is most conveniently described as electron diffusion across a linear concentration gradient. However, it can equivalently be described as electron migration across a varying potential gradient.

Another apparent difference between conducting polymers and redox polymers is that the former are conductive when dry while the latter are generally not. However, oxidized conducting polymers are generally obtained in a mixed-valent state (most are unstable when fully oxidized), while dry redox polymers are generally obtained in a single oxidation state. Mixed-valent dry redox polymers are electronic conductors.[16]

Finally, it is interesting to note that the conductivity of polypyrrole remains at electrochemically useful levels at potentials as low as –0.8 V vs SSCE in acetonitrile. Further, in the potential region between ca. –0.8 and –0.4 V it exhibits useful conductivity but little charging current. This would therefore be the optimum region in which to use polypyrrole for analytical voltammetry. Since such a region will occur at different potentials for other polymers (it is centered at ca. +0.5 V for poly-MPMP$^+$), the appropriate polymer for a particular analysis could be selected on this basis.

Acknowledgment. Financial support from the Natural Sciences and Engineering Research Council of Canada (NSERC) and Memorial University is gratefully acknowledged. We also thank Royce Murray for helpful comments on this manuscript.

(39) Chidsey, C. E. D.; Murray, R. W. *J. Phys. Chem.* **1986**, *90*, 1479–1484.

(40) Dahms, H. *J. Phys. Chem.* **1968**, *72*, 362–364.